RSC Advances

PAPER

Cite this: *RSC Adv.*, 2015, **5**, 13660

Cellular binding of nanoparticles disrupts the membrane potential†

Emilie A. K. Warren and Christine K. Payne*

Received 3rd December 2014
Accepted 22nd January 2015

DOI: 10.1039/c4ra15727c

www.rsc.org/advances

All cells generate an electrical potential across their plasma membrane driven by a concentration gradient of charged ions. A typical resting membrane potential ranges from −40 to −70 mV, with a net negative charge on the cytosolic side of the membrane. Maintenance of the resting membrane potential depends on the presence of two-pore-domain potassium "leak" channels, which allow for outward diffusion of potassium ions along their concentration gradient. Disruption of the ion gradient causes the membrane potential to become more positive or more negative relative to the resting state, referred to as "depolarization" or "hyperpolarization," respectively. Changes in membrane potential have proven to be pivotal, not only in normal cell cycle progression but also in malignant transformation and tissue regeneration. Using polystyrene nanoparticles as a model system, we use flow cytometry and fluorescence microscopy to measure changes in membrane potential in response to nanoparticle binding to the plasma membrane. We find that nanoparticles with amine-modified surfaces lead to significant depolarization of both CHO and HeLa cells. In comparison, carboxylate-modified nanoparticles do not cause depolarization. Mechanistic studies suggest that this nanoparticle-induced depolarization is the result of a physical blockage of the ion channels. These experiments show that nanoparticles can alter the biological system of interest in subtle, yet important, ways.

1 Introduction

All cells maintain an electrical potential across their plasma membrane driven by a concentration gradient of charged ions.[1–3] The resting state of this membrane potential is characterized by a net negative charge on the cytosolic side of the membrane. This electrochemical difference is driven by the action of sodium/potassium (Na^+/K^+) pumps, which generate a relatively high intracellular K^+ concentration. As K^+ ions diffuse out of the cell through K^+ ion leak channels, the cell interior becomes effectively negative relative to the increasingly positive exterior. Disruption of this gradient can lead to a more positive or more negative membrane potential relative to the resting state, referred to as "depolarization" or "hyperpolarization," respectively.

For all cell types, membrane potential plays a key role in cellular proliferation and differentiation.[4–6] For example, during cell cycle progression, changes in membrane potential follow regular patterns: cells entering the S phase become hyperpolarized, while in the M phase they become depolarized.[7,8] Overall, non-proliferating cells such as muscle cells and neurons have hyperpolarized membrane potentials. In comparison, actively proliferating cells are highly depolarized.[5,9] This highly proliferative group includes not only embryonic and undifferentiated stem cells but also cancer cells. Intracellular electrical recordings carried out *in vitro* and *in vivo* show that cancer cells are depolarized relative to healthy cells of the same tissue.[7,10] In a similar way, programmed changes in membrane potential are coupled to tissue regeneration following injury. *Xenopus* tadpoles depend on a sequence of depolarization followed by hyperpolarization to regenerate severed tails.[6,11,12] These observations indicate that controlling membrane potential may provide a method to control cancer or regenerate tissue. They also suggest that unintended changes to membrane potential may have significant biological implications.

Our goal was to determine if the cellular binding of nanoparticles (NPs) affected membrane potential. NPs used in diagnostic and therapeutic applications are treated as inert probes or delivery vehicles.[13–20] While the NP-delivered drug is expected to alter a cell, it is assumed that the NP itself will not change the biological system of interest.[21,22] Previous research from our lab had shown that the cellular binding of NPs is affected by membrane potential;[23] our current studies address the opposite question to determine if NPs alter the membrane potential. Using both fluorescence microscopy and flow

School of Chemistry and Biochemistry and Parker H. Petit Institute for Bioengineering and Bioscience, Georgia Institute of Technology, 901 Atlantic Drive, Atlanta, Georgia, 30332. E-mail: christine.payne@chemistry.gatech.edu; Tel: +995 404 385 3125

† Electronic supplementary information (ESI) available: Table of hydrodynamic diameters, confocal images of nanoparticle binding at 4 °C, nanoparticle concentration-dependent binding, depolarization in response to 200 nm nanoparticles, results for carboxylate-modified nanoparticles and HeLa cells. See DOI: 10.1039/c4ra15727c

cytometry, we measured relative changes in membrane potential in response to the cellular binding of NPs. For cells treated with 50 nm or 200 nm amine-modified polystyrene NPs, we observed depolarization, independent of cell type. Similar results were obtained previously with 10 nm gold NPs, although NP binding was not distinguished from internalization.[24] We then probed the mechanism that leads to NP-induced depolarization. Measuring the activity of potassium channels, we observed a significant reduction in channel permeability following the cellular binding of NPs, suggesting that the NPs physically block the potassium ion channels responsible for maintaining the resting membrane potential. Our results show that even "inert" NPs can alter the resting membrane potential of cells. This is especially important for diagnostics and therapeutics that utilize NPs as tools to probe or deliver cargo to biological systems. For future nanomedicine applications, we must consider NPs as active species able to selectively generate cellular responses.

2 Experimental

2.1 Cell culture

CHO-K1 cells (ATCC, Manassas, VA) were maintained in a 37 °C, 5% carbon dioxide environment in Ham's F-12 medium (21700-075, Invitrogen, Grand Island, NY) supplemented with 10% (v/v) fetal bovine serum (FBS, 10437-028, Invitrogen). HeLa cells (ATCC) were maintained in a 37 °C, 5% carbon dioxide environment in Minimum Essential Medium (MEM, 61100-061, Invitrogen) supplemented with 10% (v/v) FBS. Cells were passaged every 3–4 days, with replacement of the culture medium on the second day after passage.

2.2 Nanoparticles (NPs)

Polystyrene NPs were used as a model system for all experiments. For the majority of flow cytometry and fluorescence microscopy experiments, 50 nm red-fluorescent (Ex/Em: 527/570 nm) amine-modified (cationic) NPs (AMFR-050NM, Magsphere, Pasadena, CA) and carboxylate-modified (anionic) NPs (CAFR-050NM, Magsphere) were used. For propidium iodide (PI) assays, 50 nm yellow-green-fluorescent (Ex/Em: 488/509 nm) NPs (AMYF-050NM, Magsphere) were used. For LDH release and potassium channel activity assays, 58 nm non-fluorescent ('dark') amine-modified NPs (PA02N, Bangs Laboratories, Fishers, IN) were used. To test the effect of NP diameter, additional flow cytometry and PI experiments were carried out using 200 nm amine-modified NPs (A37356, Invitrogen). Dark NPs were chosen over fluorescent ones for assays in which absorbance or emission from the NP would overlap with the signal of interest. The concentration of NPs used in each experiment was calculated using the particle diameter provided by the supplier and expressed as a molarity with each particle treated as a molecule.

Many of the NPs used in these experiments have a larger hydrodynamic diameter than the value reported by the supplier, which is often obtained by electron microscopy. Throughout the text, we use the value reported by the supplier to denote the NP. The hydrodynamic diameters are listed in the ESI (Table S1†). For example, the 50 nm amine-modified NPs and 200 nm amine-modified NPs used in the depolarization experiments have a hydrodynamic diameter of 60 nm and 270 nm respectively, measured by dynamic light scattering (Nano-ZS, Malvern Instruments, Worcestershire, UK) in water.

2.3 Measurement of membrane potential

A slow-response, potential-sensitive, bis-oxonol fluorophore, $DiBAC_4(3)$ (B-438, Invitrogen), was used to measure the relative membrane potential of cells.[25–29] Cells were incubated with 20 nM DiBAC for 10 minutes at 4 °C. When DiBAC enters the cell, it binds to intracellular proteins and lipid membranes, resulting in enhanced fluorescence (Ex/Em: 490/516 nm). As the membrane potential becomes more positive, or depolarizes, cells become increasingly more permeable to DiBAC, indicated by increased fluorescence. Conversely, a more negative, or hyperpolarized, membrane potential is indicated by a decrease in fluorescence. The change in DiBAC intensity was monitored by flow cytometry (Accuri C6, Becton Dickinson, Franklin Lakes, NJ) and fluorescence microscopy (Olympus IX71, FITC filter). For NP-induced depolarization experiments, DiBAC was added to cells after NP incubation and centrifugation. This prevents the interaction of the NPs with DiBAC that can lead to imaging artifacts.

2.4 Flow cytometry

The CHO and HeLa cells used for these experiments are adherent cells that grow on the surface of cell culture flasks or dishes. For flow cytometry, these cells were removed from the surface of the culture flasks using Accutase (A6964, Sigma Aldrich, Milwaukee, WI). After removal from the cell culture flask, the suspension of cells was split into eight 1 mL aliquots in Eppendorf tubes. Each aliquot of cells was then pelleted (5000 rcf for 7 minutes) and resuspended in ice-cold PBS. Cationic or anionic NPs were added to half of the cells (5–150 pM). Cell samples in the absence of NPs were used as controls. All samples were incubated at 4 °C for 10 minutes, followed by centrifugation (2000 rcf for 5 min) and resuspension in PBS. Each sample was treated with 20 nM DiBAC, incubated for another 10 minutes at 4 °C, and washed (2000 rcf for 5 min, resuspend in PBS). The cell suspensions were then filtered (40 μm nylon filter) for flow cytometry. Flow cytometry was carried out using a BD Accuri C6 flow cytometer. The polystyrene NPs are embedded with a red-fluorescent dye and detected by the FL-2 filter (585/40 BP). DiBAC fluorescence was detected by the FL-1 filter (533/30 BP). For each experiment, ≈15 000 cells in the population of interest (determined by a propidium iodide assay) were sampled. Histograms were analyzed using the BD Accuri C6 software. The percent change between the mean DiBAC intensity of quadruplicate control samples and that of quadruplicate NP-treated samples was used to measure relative shifts in membrane polarization. Day to day variability of cell samples is accounted for by calculating percent change, rather than comparing the absolute values. A p-value of <0.05 was used as a threshold to determine significance of changes in mean intensity.

2.5 Fluorescence microscopy

For fluorescence imaging, cells were cultured in 35 mm glass-bottom cell culture dishes (MatTek, Ashland, MA). Cells were treated as described for flow cytometry, although remaining adhered to the glass coverslip for imaging experiments. First, the nuclei of the cells were stained with 36 μM 4′,6-diamidine-2-phenylindole dilactate (DAPI, D3571, Invitrogen) at 37 °C for 25 minutes in the existing culture medium. The cells were then rinsed with cold PBS, treated with NPs for 10 minutes at 4 °C, and rinsed again immediately prior to imaging to remove any unbound NPs. For some experiments, which are noted, cells were instead incubated with 200 nM DiBAC for 10 minutes before imaging. The cells were imaged with an epifluorescence microscope (Olympus 1X71, Center Valley, PA) using a 1.20 N.A., 60×, water immersion objective (Olympus). Emission was detected with an EMCCD camera (DU-897, Andor, South Windsor, CT). All images for comparison were acquired with the same exposure time and gain. Image J (http://rsb.info.nih.gov/ij/) was used for analysis. For comparison, brightness and contrast were set equally for all images.

2.6 Membrane permeabilization assays

The degree to which NPs induce membrane permeabilization and cell death was tested using both propidium iodide (PI, P1304MP, Invitrogen) and lactate dehydrogenase (LDH, 88953, Pierce Biotechnology, Rockford, IL) assays.

For a PI assay, the cells were prepared for flow cytometry as described previously. After NP addition and wash, the cells were resuspended in PBS containing 2 μg mL^{-1} PI and incubated at 4 °C for 15 minutes. The samples were then filtered and run on the flow cytometer. Any cells exhibiting a strong fluorescence signal on the FL-2 filter were considered dead, as PI only enters dead cells. The percentage of live cells with intact membranes was calculated by dividing the number of dead cells by the total population and subtracting that value from 100. Standard deviations were calculated from quadruplicate measurements of each condition.

For a LDH assay, cells were passaged into a 24-well plate at 100 000 cells per well in complete culture medium and allowed to grow for 24 hours. Prior to the experiment, the plate was cooled on ice for 15–20 minutes. The medium in the wells was replaced with PBS and dark (non-fluorescent) NPs were added for an incubation of 10 minutes at 4 °C. As controls, sets of triplicate wells were treated only with water ("Spontaneous LDH") or with 10× lysis buffer ("Max LDH"). Without rinsing off excess NPs, the plate was then moved to a 37 °C environment to incubate for 45 minutes. After this incubation step, 50 μL of solution from each well was transferred to a clear 96-well plate. To each of these solutions, 50 μL of the reaction mixture (provided in the assay kit) was added and incubated, covered, at room temperature for 30 minutes. Finally, 30 μL of stop solution (also provided in the kit) was added to each well, and the absorbance at 490 nm and 680 nm was measured on a microplate reader (SpectraMax M2e, Molecular Devices, Sunnyvale, CA). LDH activity was determined by subtracting the 680 nm absorbance value (background) from the 490 nm reading. Percent cytotoxicity was calculated by [(LDH activity − spontaneous LDH activity)/(max LDH activity − spontaneous LDH activity)] × 100. For both PI and LDH assays, a p-value of <0.05 was used as a threshold to determine significance of changes in activity.

2.7 Depolarization of cells with extracellular K^+

Cells were depolarized independently of NPs by incubating them with phosphate buffered saline (PBS) solutions in which Na^+ salts were replaced with K^+ salts. The addition of extracellular K^+ decreases the K^+ flux across the membrane and has been shown previously to depolarize cells.[30,31] The control PBS solution (14040, Invitrogen) contains 4 mM K^+ ions. Depolarizing solutions were prepared with 10 mM K^+ to 140 mM K^+. We refer to these solutions by their K^+ concentration: "PBS K-10" refers to the solution with 10 mM K^+. Cells were treated for 10 minutes with the PBS K solution at 4 °C.

2.8 Potassium channel activity

To measure the activity of cellular potassium channels, a Thallos assay (0910, TEFLabs, Austin, TX) was used. This assay measures the permeability of potassium channels based on the ability of thallium ions to pass through them. Cells cultured on a 24-well plate were loaded with a thallium-sensitive dye over a 1 hour incubation at 37 °C. To determine if NPs affect the permeability of potassium channels, the plate was cooled to 4 °C on ice over 15–20 minutes, and dark (non-fluorescent) NPs were added to the cells for an additional 10 minutes. The baseline fluorescence intensity (Ex/Em: 490/515 nm) of each well was recorded for 5 minutes at 30 second intervals on a microplate reader. Then, 100 μL of a 5 mM thallium sulfate solution was added to each well. As thallium ions enter the cell through potassium channels, they bind to the intracellular dye, resulting in fluorescence. This increase in fluorescence intensity was measured for 60 minutes at 30 second intervals.

The raw fluorescence data for the control and each experimental condition was averaged over 4 wells. The increase in fluorescence intensity from the baseline, F/F_0, was calculated by normalizing each data point against its respective average baseline value. Representing the data this way minimized differences in the baseline and raw intensity values between days and cell samples. The amount of Tl^+ uptake was determined by dividing each experimental value by the control value at 660 seconds, the time point of maximum difference. Fig. 4 shows data collected from a single experiment on a 24-well plate. Experiments performed in separate well plates on other days showed similar trends.

3 Results and discussion

3.1 Cellular binding of amine-modified NPs leads to depolarization

We first examined the binding of 50 nm amine-modified polystyrene NPs to Chinese hamster ovary (CHO) cells. In order to study the effects of NPs binding to the plasma membrane, independent of internalization, all experiments were conducted

at 4 °C to block endocytosis (Fig. S1†).[32,33] The polystyrene NPs are embedded with a red fluorophore (Ex/Em: 527/570 nm), allowing us to detect cellular binding using both fluorescence microscopy and flow cytometry. For both types of experiments, cells were treated with NPs (5–150 pM) for 10 minutes, as described in Experimental. Cellular binding of NPs was visible at all NP concentrations tested (Fig. 1A and B), with increased NP fluorescence as a function of NP concentration (Fig. S2†).

Using flow cytometry, we monitored the effect of NP binding on cellular membrane potential using the mean fluorescence intensity of DiBAC (20 nM, 10 min incubation following NP incubation) as a relative measure of depolarization. Increased DiBAC signal corresponds to a more positive, or depolarized, membrane potential. For each flow cytometry experiment, quadruplicate samples were measured. Changes in the membrane potential in response to NP binding were characterized as the percent change in DiBAC fluorescence intensity relative to the control. Flow cytometry showed that the addition of 5 pM amine-modified NPs led to a 33% increase in DiBAC fluorescence compared to the control, indicating membrane depolarization in response to NP binding (Fig. 1C). Increasing concentrations of NPs led to increased depolarization. At 50 pM NPs, we observed a plateau in depolarization with no significant difference observed following incubation with 150 pM NPs.

Depolarization was also observed following cellular binding of 200 nm NPs. CHO cells treated with 200 nm amine-modified NPs at a concentration of 50 pM exhibited a 53% greater DiBAC fluorescence signal than control cells in the absence of NPs (Fig. S3†). In a previous study, a similar depolarization was observed with 10 nm cationic gold NPs; however, these experiments did not distinguish between NP binding and internalization.[24] Future work will examine depolarization as function of NP diameter. In comparison to the amine-modified NPs, repeated experiments with 50 nm carboxylate-modified polystyrene NPs (5–480 pM) showed no significant trend in depolarization (Fig. S4†).

To determine if the observed depolarization in response to amine-modified NPs was cell type dependent, fluorescence microscopy and flow cytometry experiments were repeated using human cervical carcinoma (HeLa) cells. The same general trend was observed: cellular binding of amine-modified NPs to HeLa cells led to depolarization with increased depolarization at higher NP concentrations (Fig. S5†).

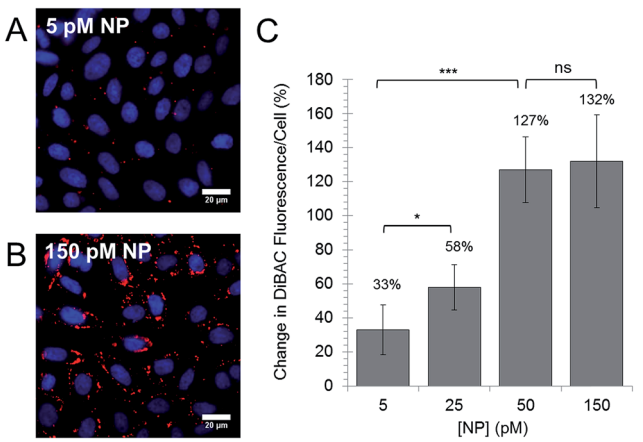

Fig. 1 Cellular binding of NPs leads to increased internalization of DiBAC. (A) Fluorescence microscopy image of CHO cells incubated with 5 pM of 50 nm amine-modified NPs (red) for 10 minutes at 4 °C. Nuclei were stained with DAPI (blue). (B) Increased concentrations of NPs lead to increased binding (Fig. S2†). (C) Flow cytometry was used to measure the internalization of DiBAC (20 nM). Data show the percentage increase in DiBAC intensity per cell compared to a control in the absence of NPs. Values are the average of quadruplicate measurements. Error bars show standard deviation. ns = not significant, * $p < 0.05$, *** $p < 0.001$.

3.2 Cellular binding of NPs does not result in membrane permeabilization

Permeabilization of the plasma membrane could account for increased DiBAC fluorescence, independent of changes to the membrane potential. This is especially true with the amine-modified NPs, as it has been shown that cationic NPs are more cytotoxic than anionic or neutral NPs.[34–37] This toxicity is associated with damage to the plasma membrane, possibly due to electrostatic interaction between the amino groups of the NP and the phospholipids of the membrane, leading to a disruption of the lipid bilayer.[36] In previous studies of NP-induced depolarization, injury to the cell membrane was evaluated by transmission electron microscopy (TEM) images, with no damage detected.[24] As a more sensitive measure of membrane permeabilization, we applied two standard tests that assess membrane disruption under normal physiological conditions: a propidium iodide (PI) assay and a lactate dehydrogenase (LDH) release assay.

PI is a membrane impermeant molecule that, while excluded from viable cells, can be internalized through the holes of a damaged cell membrane. Upon entering the cell, PI binds to DNA and exhibits an enhanced red fluorescence. Using flow cytometry, we measured the number of PI-positive CHO cells to quantify the population of cells with permeabilized membranes. With the addition of 50 nm amine-modified NPs, the only significant decrease in percentage of live cells with intact plasma membranes was observed upon addition of 150 pM NPs, with a 4% decrease of live cells (Fig. 2A). This decrease is likely too small as to account for the 132% increase in DiBAC signal occurring at this NP concentration (Fig. 1C). The larger 200 nm NPs caused significant membrane permeabilization at concentrations greater than 50 pM (Fig. S6†).

The LDH release assay measures the degree to which LDH, a cytosolic enzyme present in many different cell types, leaks from the cell due to membrane damage.[38] The amount of LDH that leaks into the extracellular medium can be quantified by a coupled enzymatic reaction that colorimetrically indicates the amount of LDH present. With treatment of up to 150 pM NPs, there was no significant increase in the amount of LDH released from the CHO cells (Fig. 2B).

At 50 nm NP concentrations above 150 pM, the expected cytotoxic effects of amine-modified NPs were observed. At 600 pM NPs, the PI assay indicated that greater than 50% of the

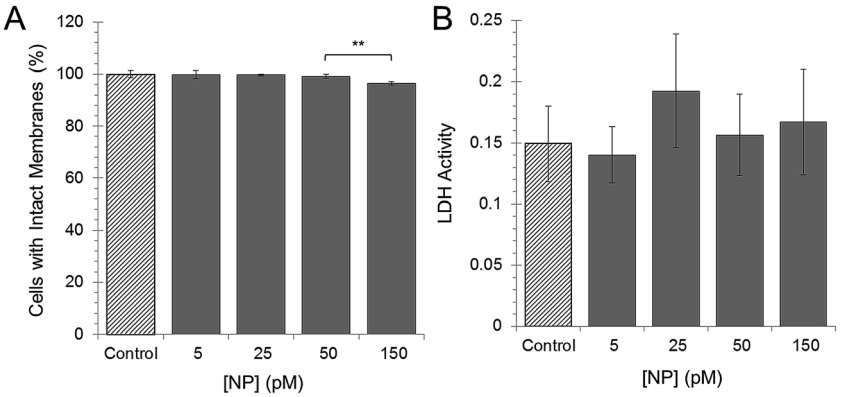

Fig. 2 NPs do not permeabilize the cell membrane at low concentrations. (A) Propidium iodide (PI) staining of CHO cells was used to measure the percentage of live cells with intact membranes following incubation with 50 nm amine-modified NPs. Data is normalized against the control in the absence of NPs. $n = 4$, ** $p < 0.01$ (B) An assay of LDH activity shows no significant increase in extracellular LDH in response to NP binding. $n = 6$. Error bars show standard deviation.

cells in the sample were dead (data not shown). Significant LDH release occurred at 1 nM NPs (data not shown).

3.3 Pre-depolarization of cells with extracellular K^+ diminishes NP-induced depolarization

Maintenance of the resting membrane potential depends on the presence of two-pore-domain potassium "leak" channels, which allow for outward diffusion of potassium ions along their concentration gradient.[3,39] A common way to induce depolarization is by increasing the extracellular concentration of potassium. The additional extracellular K^+ decreases the K^+ flux across the membrane through these leak channels, causing accumulation of positive charge inside the cell.[40] We prepared phosphate buffered saline (PBS) solutions with elevated levels of K^+. Standard PBS contains 4 mM K^+; the depolarizing "PBS K" solutions contained 10–100 mM K^+. In order to test whether depolarization with NPs is additive, we incubated the cells in depolarizing solution before NP treatment and DiBAC addition.

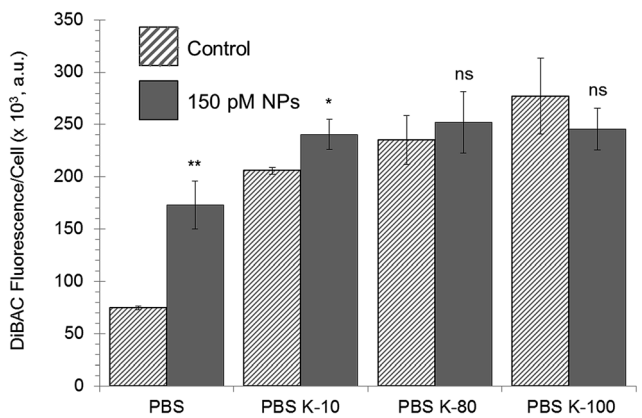

Fig. 3 Pre-incubation of cells with extracellular potassium decreases the depolarizing effect of NPs (150 pM, 50 nm, amine-modified). At 80 mM potassium (PBS K-80) and greater, the addition of NPs no longer leads to depolarization. Control experiments with PBS are re-plotted from Fig. 1. Error bars show standard deviation, $n = 4$. ns = not significant, * $p < 0.05$, ** $p < 0.01$.

The relative membrane potential was measured using flow cytometry. In control PBS, NP-treated cells (150 pM) showed a 132% increase in DiBAC fluorescence compared to cells in the absence of NPs (Fig. 3). However, after initial depolarization with PBS containing 10 mM K^+, cells that were subsequently treated with NPs exhibited only a 17% increase in DiBAC fluorescence from the control. Upon further increase of the extracellular K^+ concentration—to 80 and 100 mM—there was no longer a significant change between the control and NP-treated samples.

3.4 NPs depolarize cells by blocking potassium channels

Since pre-depolarization with PBS K buffers reduces the depolarization capability of subsequent NP treatment, it suggests that the NPs alter the membrane potential in the same way: by decreasing the K^+ flux across the membrane. We propose that NPs physically block the potassium ion channels responsible for maintaining the resting potential. Prevention of potassium ion efflux due to blocked channels causes accumulation of positive charge inside the cell, resulting in a depolarized membrane. To test this mechanism, we used an assay that assesses the permeability of potassium channels based on diffusion of thallium ions through the channels. Internalized thallium then activates a fluorescent dye pre-loaded into the cytosol of the cells. Fluorescence measurements were recorded over a 65 minute period (5 minutes for baseline, 60 minutes for Tl^+ addition). Fluorescence intensities reached a maximum and plateaued at ~35 minutes (2100 seconds) for all samples. Triplicate experiments repeated over different days yielded the same results: Tl^+-activated fluorescent signal decreases with increasing concentration of NPs (Fig. 4A). While there is no significant change in Tl^+ uptake with 5 pM NP treatment, uptake steadily decreases down to 79% with 150 pM NPs six minutes after Tl^+ addition ($t = 660$ seconds) (Fig. 4B). At this time, the difference in Tl^+ uptake is greatest. These results directly relate the presence of membrane-bound NPs to a loss in potassium channel permeability.

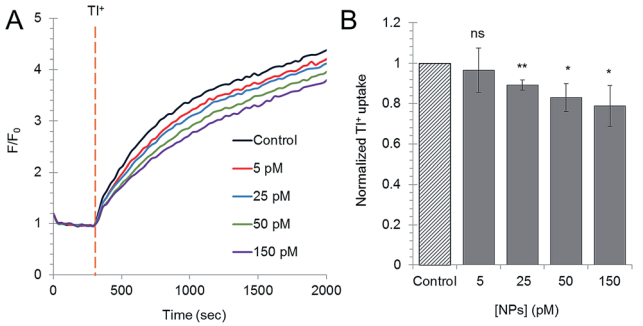

Fig. 4 Cellular binding of NPs decreases the permeability of potassium channels. (A) Intracellular fluorescence of a Tl^+-sensitive dye was measured following the addition of extracellular Tl^+ (vertical orange dashed line). (B) Difference in Tl^+ internalization at $t = 660$ seconds. Internalization is normalized against the control. Error bars show standard deviation, $n = 4$. ns = not significant, * $p < 0.05$, ** $p < 0.01$ (relative to control).

4 Conclusion

Using flow cytometry and fluorescence microscopy, we found that the cellular binding of amine-modified NPs leads to the depolarization of CHO and HeLa cells (Fig. 1, S3 and S5†). Similar results have been reported previously using 10 nm cationic gold NPs.[24] This prior study monitored the downstream effects of NP internalization: increased levels of intracellular calcium, reduced proliferation, and increased apoptosis. In comparison, we have isolated the initial binding of NPs to the plasma membrane in order to examine the underlying mechanism that leads to depolarization. We show that the NPs do not permeabilize the plasma membrane (Fig. 2), but instead lead to depolarization by interfering with the potassium channels that are responsible for maintaining the resting membrane potential (Fig. 3 and 4). Future studies will address three specific questions using a combination of experiments and modeling:[41] (1) the relationship between NP diameter and depolarization (Fig. S3†), (2) the differences in cellular binding between amine-modified NPs and carboxylate-modified NPs (Fig. S4†), and (3) NP binding, NP internalization, and depolarization at 37 °C. Overall, these experiments show that NPs used in biological applications can alter the system of interest in unexpected ways and that cytotoxicity alone is not a measure of perturbation. In addition, our results suggest a future application of NPs as tools to control membrane potential, thereby controlling cell proliferation,[4–6] malignant transformation,[7,10] and tissue regeneration.[6,11,12]

Acknowledgements

The authors acknowledge support from a NIH Director's New Innovator Award (1DP2OD006470) to C.K.P.

Notes and references

1 B. Alberts, D. Bray, J. Lewis, M. Raff, K. Roberts and J. D. Watson, *Molecular Biology of the Cell*, New York, Garland Pub., 1989.
2 I. M. Glynn and S. J. D. Karlish, *Annu. Rev. Physiol.*, 1975, **37**, 13.
3 S. A. N. Goldstein, D. Bockenhauer, I. O'Kelly and N. Zilberberg, *Nat. Rev. Neurosci.*, 2001, **2**, 175.
4 S. Sundelacruz, M. Levin and D. L. Kaplan, *Stem Cell Rev. Rep.*, 2009, **5**, 231.
5 M. Levin, *BioEssays*, 2012, **34**, 205.
6 M. Levin, *Semin. Cell Dev. Biol.*, 2009, **20**, 543.
7 M. Yang and W. J. Brackenbury, *Front. Physiol.*, 2013, **4**, 185.
8 W. F. Wonderlin and J. S. Strobl, *J. Membr. Biol.*, 1996, **154**, 91.
9 R. Binggeli and R. C. Weinstein, *J. Theor. Biol.*, 1986, **123**, 377.
10 A. A. Marino, I. G. Iliev, M. A. Schwalke, E. Gonzalez, K. C. Marler and C. A. Flanagan, *Tumor Biol.*, 1994, **15**, 82.
11 D. S. Adams, A. Masi and M. Levin, *Development*, 2007, **134**, 1323.
12 A.-S. Tseng and M. Levin, *Anat. Rec.*, 2012, **295**, 1541.
13 M. De, P. S. Ghosh and V. M. Rotello, *Adv. Mater.*, 2008, **20**, 4225.
14 A. P. Alivisatos, W. W. Gu and C. Larabell, *Annu. Rev. Biomed. Eng.*, 2005, **7**, 55.
15 D. S. Kohane, *Biotechnol. Bioeng.*, 2007, **96**, 203.
16 D. A. Giljohann, D. S. Seferos, W. L. Daniel, M. D. Massich, P. C. Patel and C. A. Mirkin, *Angew. Chem., Int. Ed.*, 2010, **49**, 3280.
17 X. Michalet, F. F. Pinaud, L. A. Bentolila, J. M. Tsay, S. Doose, J. J. Li, G. Sundaresan, A. M. Wu, S. S. Gambhir and S. Weiss, *Science*, 2005, **307**, 538.
18 E. M. Pridgen, R. Langer and O. C. Farokhzad, *Nanomedicine*, 2007, **2**, 669.
19 S. J. Rosenthal, J. C. Chang, O. Kovtun, J. R. McBride and I. D. Tomlinson, *Chem. Biol.*, 2011, **18**, 10.
20 E. C. Dreaden, A. M. Alkilany, X. Huang, C. J. Murphy and M. A. El-Sayed, *Chem. Soc. Rev.*, 2012, **41**, 2740.
21 E. E. Connor, J. Mwamuka, A. Gole, C. J. Murphy and M. D. Wyatt, *Small*, 2005, **1**, 325.
22 R. Kumar, I. Roy, T. Y. Ohulchanskky, L. A. Vathy, E. J. Bergey, M. Sajjad and P. N. Prasad, *ACS Nano*, 2010, **4**, 699.
23 E. H. Shin, Y. Li, U. Kumar, H. V. Sureka, X. Zhang and C. K. Payne, *Nanoscale*, 2013, **5**, 5879.
24 R. R. Arvizo, O. R. Miranda, M. A. Thompson, C. M. Pabelick, R. Bhattacharya, J. D. Robertson, V. M. Rotello, Y. S. Prakash and P. Mukherjee, *Nano Lett.*, 2010, **10**, 2543.
25 T. Klapperstueck, D. Glanz, M. Klapperstueck and J. Wohlrab, *Cytometry, Part A*, 2009, **75**, 593.
26 E. B. George, P. Nyirjesy, P. R. Pratap, J. C. Freedman and A. S. Waggoner, *J. Membr. Biol.*, 1988, **105**, 55.
27 V. DallAsta, R. Gatti, G. Orlandini, P. A. Rossi, B. M. Rotoli, R. Sala, O. Bussolati and G. C. Gazzola, *Exp. Cell Res.*, 1997, **231**, 260.
28 A. S. Waggoner, *Annu. Rev. Biophys. Bioeng.*, 1979, **8**, 47.
29 J. Plasek and K. Sigler, *J. Photochem. Photobiol., B*, 1996, **33**, 101.
30 J. B. Rothbard, T. C. Jessop, R. S. Lewis, B. A. Murray and P. A. Wender, *J. Am. Chem. Soc.*, 2004, **126**, 9506.

31 D. Terrone, S. L. W. Sang, L. Roudaia and J. R. Silvius, *Biochemistry*, 2003, **42**, 13787.
32 I. H. Pastan and M. C. Willingham, *Science*, 1981, **214**, 504.
33 C. Szymanski, H. Yi, J. Liu, E. Wright and C. Payne, in *NanoBiotechnology Protocols*, ed. S. J. Rosenthal and D. W. Wright, Humana Press, 2013, vol. 1026, ch. 2, p. 21.
34 N. Lewinski, V. Colvin and R. Drezek, *Small*, 2008, **4**, 26.
35 T. Xia, M. Kovochich, M. Liong, J. I. Zink and A. E. Nel, *ACS Nano*, 2008, **2**, 85.
36 C. M. Goodman, C. D. McCusker, T. Yilmaz and V. M. Rotello, *Bioconjugate Chem.*, 2004, **15**, 897.
37 A. Verma and F. Stellacci, *Small*, 2010, **6**, 12.
38 T. Decker and M. L. Lohmann-Matthes, *J. Immunol. Methods*, 1988, **115**, 61.
39 P. Enyedi and G. Czirjak, *Physiol. Rev.*, 2010, **90**, 559.
40 C. Callies, J. Fels, I. Liashkovich, K. Kliche, P. Jeggle, K. Kusche-Vihrog and H. Oberleithner, *J. Cell Sci.*, 2011, **124**, 1936.
41 S. Mukhopadhyay, F. Zhang, E. Warren and C. Payne, *53rd IEEE Conference on Decision and Control*, 2014.